Special Issue on Metamaterials LHM

At and below the Chu limit: passive and active broad bandwidth metamaterial-based electrically small antennas

R.W. Ziolkowski and A. Erentok

Abstract: The solution to the canonical problem of a radiating infinitesimal electric dipole antenna that is centred in a multilayered, concentric metamaterial-based spherical shell system is presented. It is demonstrated that when this system is electrically small, a specifically designed homogenous and isotropic epsilon-negative (ENG) layer can function as a distributed matching element to the antenna enabling a resonant radiation behaviour. A finite element model of the corresponding centre-fed cylindrical dipole antenna-based resonant system confirms that such designed ENG-based spherical layers can act as a distributed matching element, which can be optimised to produce a reactance free, resistively matched and, hence, efficient radiating system. Several limits on the dispersion properties of the homogenous and isotropic ENG media used in these matching layers are considered and their impact on the bandwidth of these resonant systems is established. Although the dispersionless resonant antenna–ENG system has a bandwidth substantially below the Chu limit, the bandwidths of the corresponding dispersive systems are shown to be at or just slightly below the Chu limit. An analytical model of an idealised gaseous plasma-based ENG layer sandwiched between two glass layers, a potential realisation of these metamaterial-based ENG spherical shell systems, is introduced and its solution is used to study these efficiency and bandwidth issues further. Resonant systems based on active ENG metamaterial layers realised with two types of idealised gain medium models are shown to have bandwidths that approach the idealised dispersionless medium values and, consequently, are substantially below the Chu limit.

1 Introduction

An electrically small dipole antenna is known to be a very inefficient radiator [1–8], that is, because it has a very small radiation resistance while simultaneously having a very large capacitance reactance, a very large impedance mismatch to any realistic power source exists. A wide variety of approaches to achieve matched systems have been proposed. For example, by including an inductor to achieve conjugate matching and a quarter-wave transformer to achieve resistance matching, one can obtain complete matching of an electrically small antenna to a source. Although the entire matching network-antenna system is not electrically small, the end result is an efficient radiator. A different paradigm was proposed recently [9–11]. By surrounding an electrically small antenna in a metamaterial environment, such as an electrically small electric dipole antenna in an electrically small homogenous, isotropic and dispersionless double negative (DNG) or an epsilon-negative (ENG) shell, complete resistive and reactive matching and, hence, an efficient electrically small radiating system was achieved.

In the work of Ziolkowski and Erentok [11], the analytical solution of a three-region antenna problem, which consisted of an infinitesimal electric dipole in free space enclosed in a spherical ENG shell, was used to study the behaviour of such metamaterial-based electrically small antenna systems. A naturally resonant configuration was obtained by combining an electrically small inductive ENG shell (a capacitive element with a properly designed negative permittivity and thickness) with the capacitive, electrically small radiating element. More realistic electrically small antenna systems formed by combining a centre-fed, finite radius cylindrical electric dipole with an ENG spherical shell and a coaxially fed electric monopole over an infinite ground plane with a hemispherical ENG shell were also modelled numerically using ANSOFT's high frequency structure simulator (HFSS). These numerical models provided the input resistance and reactance of these realistic antenna–ENG shell systems. It was demonstrated that electrically small versions of these realistic antenna systems could be designed to have a zero input reactance and an input resistance that is matched to a specified source to yield a very high overall efficiency (total power radiated essentially equal to the source input power). Their far-field radiation patterns corresponded to those of the constituent antenna radiating into free space.

The bandwidths of these metamaterial-based antenna systems were also considered analytically. It was demonstrated that if the ENG shell was treated as a hypothetical frequency-independent medium, the predicted fractional bandwidths were significantly larger than those predicted by the Chu limit [1–8]. On the other hand, it was also shown that if the more realistic dispersion properties of the ENG shell were included, the high overall efficiency remained at the operating frequency but the fractional bandwidths were reduced significantly, but still being

doi:10.1049/iet-map:20050342

Paper first received 6th December 2005 and in revised form 30th June 2006

The authors are with the Department of Electrical and Computer Engineering, University of Arizona, 1230 E. Speedway Blvd., Tucson, AZ 85721-0104, USA

E-mail: ziolkows@ece.arizona.edu

slightly larger than the Chu limit. Because these fractional bandwidths were very small, these dispersion-bandwidth studies were performed with the analytical models rather than the numerical ones. The procedure to extract bandwidth values from the total radiated power predicted by the analytical models that agreed with those obtained with the input impedance predicted by the numerical models was established [11].

Because of its potentially large number of practical applications, the desired goal of this metamaterial-based antenna research is to achieve a broad bandwidth, efficient and electrically small antenna system. To this end, we first establish the theoretical bounds on the dispersive properties of a passive metamaterial and then relate these bounds to the quality factor and bandwidth properties of the infinitesimal electric dipole–ENG spherical shell system and the coax-fed electric monopole–ENG hemispherical shell system. As in the previous investigations [9–11], the metamaterial-based ENG layers considered throughout this paper are assumed to be isotropic and homogeneous. It is demonstrated that a passive dispersive metamaterial cannot be used to recover the large bandwidths predicted by the non-dispersive designs. Nonetheless, quality factors slightly above and below the Chu limit are demonstrated with the dispersion-limit models. On the other hand, because we are interested in possible physical realisations of this system, in this paper we also extend the analytical model to a metamaterial-based spherical covering of an electrically small dipole antenna which includes multiple layers. In particular, we will consider the analytical and numerical models of an electron plasma enclosed in a spherical glass bottle. The plasma density and the size of the glass bottle will be specified to produce the desired negative permittivity values to achieve a resonant configuration and then a resonant antenna system, that is, we will design a metamaterial-based ENG spherical shell system that, when combined with the antenna will produce complete resistive and reactance matching to the source at the operational frequency. We again use the numerical model with the idealised metamaterials to establish the efficacy of using the analytical model to predict the bandwidth properties of the dispersive metamaterial-based systems. Because one could fill the glass bottle with a gaseous medium that has resonant states which could be excited, we will also consider an active metamaterial ENG layer in our discussion. It will be shown that the active metamaterial-based antenna system has fractional bandwidths that approach the non-dispersive limits.

As a matter of definitions to be used throughout this paper, an exp $(+j\omega t)$ time dependence is assumed throughout. An antenna in free space will be called electrically small if $ka \leq 1$, where the free space wavelength $\lambda = c/f$, f being the frequency of operation and c is the speed of light in vacuum, and $k = 2\pi/\lambda$ is the corresponding wave vector. Thus, for the target frequency of interest here, $f_0 = \omega_0/2\pi = 300$ MHz, the free space wavelength $\lambda_0 = 1.0$ m, and, consequently, the effective radius must be smaller than the Wheeler radiansphere value $a_{\max} = 1/(2\pi) = 159.15$ mm to meet this criterion. If a hemispherical geometry is considered, such as one would consider for a coaxially fed monopole through an infinite ground plane, the term electrically small means $ka \leq 0.5$ and, hence, $a_{\max,\text{hemi}} = 1/(4\pi) = 79.575$ mm. The infinitesimal electric dipole in all of the analytic cases considered below is driven with a 1.0 A current across its terminals; the more realistic numerical finite thickness centre-fed cylindrical dipole and coaxially fed cylindrical monopole antennas are driven with 1.0 W of input power from a 50 Ω or 75 Ω source.

2 Fundamental limits

2.1 Chu limit

We recall that the fundamental limits on the radiation quality factor, Q, associated with electrically small antennas have been explored by many authors [1–8]. The Q value, also defined as 2π times the ratio of the maximum energy stored to the total power lost per period, is a convenient quantity to describe, for instance, the bandwidth of the antenna when a driving circuit is matched to it. The minimum Q value attainable by an infinitesimal electric dipole, or similarly by the azimuthally symmetric TM_{10} spherical mode, has been investigated thoroughly. This minimum, that is, the Chu limit, has been shown to be (e.g. [6])

$$Q_{\text{Chu}} = \frac{1 + 2(ka)^2}{(ka)^3[1 + (ka)^2]} \tag{1}$$

where a is the radius of the radiansphere (minimum radius sphere) surrounding the antenna system and k is the wave vector for corresponding operation frequency. On the other hand, as shown in the work of McLean [6], the more exact result for the minimum quality factor is

$$Q_{\text{Exact}} = \frac{1}{(ka)^3} + \frac{1}{ka} \tag{2}$$

The difference between these expressions $|Q_{\text{Exact}} - Q_{\text{Chu}}|/|Q_{\text{Exact}}| = (ka)^4/[1 + (ka)^2]^2 \propto (ka)^4$ is very small when the system is electrically small. Consequently, for all of the comparisons made below we will use the exact expression, but we will refer to it as the Chu limit. We note that

$$Q_{\text{Exact}} \simeq \frac{1}{(ka)^3} \quad \text{for } ka \ll 1 \tag{3}$$

On the other hand, if $f_{+,3\text{ dB}}$ and $f_{-,3\text{ dB}}$ represent the frequencies above and below the resonance frequency where the radiated power falls to half its peak value, the fractional bandwidth, FBW, is related to the radiation quality factor, Q_{BW}, by the relation [8]

$$\text{FBW} = \frac{\Delta f_{3\text{dB}}}{f_{0\text{dB}}} = \frac{1}{Q_{\text{BW}}} \tag{4}$$

where the 3 dB bandwidth $\Delta f_{3\text{dB}} = f_{+,3\text{ dB}} - f_{-,3\text{ dB}} = \text{BW}$. Therefore, we can calculate the maximum fractional bandwidth based upon the Chu limit as

$$\text{FBW}_{\text{Chu}} = \frac{1}{Q_{\text{Exact}}} = \frac{(ka)^3}{[1 + (ka)^2]} \simeq (ka)^3 \quad \text{for} \quad ka \ll 1 \tag{5}$$

Consequently, as the electrical size of the dipole antenna decreases, the minimum Q value in free space increases dramatically, causing a corresponding decrease in the fractional bandwidth of the antenna system. It is commonly believed that the quality factor and the fractional bandwidth of an antenna system will approach their Chu limits only if it efficiently utilises the available volume within the radiansphere.

It is well known that the fractional bandwidth of an antenna is increased if the losses are increased, but at a cost of the total radiated power. In particular, if the radiation efficiency is η_{rad}, the quality factor and gains for the lossy and the lossless systems are related by the relations

$$Q_{\text{Lossy}} = \eta_{\text{rad}} Q_{\text{Lossless}} \tag{6}$$

$$G = \eta_{\text{rad}} D \tag{7}$$

where D is the directivity of the system. Thus, the gain–bandwidth product remains constant when comparing lossy and lossless antenna systems

$$G \times \mathrm{BW} = \eta_{\mathrm{rad}} D \times \frac{1}{\eta_{\mathrm{rad}} Q_{\mathrm{Lossless}}} = \frac{D}{Q_{\mathrm{Lossless}}} \tag{8}$$

Because all of the dipole–ENG shell systems to be considered below behave like electrically small dipole antennas, their maximum directivities are all $D \simeq 1.5$. Thus, their gain–bandwidth products can be determined essentially by the quality factor of the lossless case. Moreover, the bandwidth when losses are present in a system will always be larger than when no losses are present: $\mathrm{BW}_{\mathrm{Lossy}} = \mathrm{BW}_{\mathrm{Lossless}}/\eta_{\mathrm{rad}}$. Consequently, because they avoid any of these additional considerations, the lossless versions of the metamaterial models and the antennas were used for our investigations into the impact of dispersion on the quality factors and, hence, the bandwidths of the metamaterial-based antenna systems discussed below.

2.2 Dispersion limits

The question of what type of dispersion model, hence, metamaterial would lead to the minimum Q and, hence, the maximum fractional bandwidth performance of an electrically small metamaterial-based antenna system must be addressed. Typical restrictions on the dispersion properties of materials include energy constraints and Kramers–Krönig relations [see, for instance, 12]. We will focus on simple dispersion models that satisfy these constraints, such as the lossless Drude model

$$\varepsilon_r(\omega) = 1 - \frac{\omega_{\mathrm{p}}^2}{\omega^2} \tag{9}$$

where $\omega_{\mathrm{p}} = 2\pi f_{\mathrm{p}}$ and $\omega = 2\pi f$, f_{p} and f being the plasma frequency of the medium and the frequency of the source, respectively. However, we also wish to refine the dispersion models to achieve the minimum allowed relative epsilon variation of the dispersion properties of the ENG medium.

In all of the cases presented below, resonant systems involving only ENG metamaterials and electric dipole or monopole antennas are considered. One can achieve similar conclusions for a magnetic dipole (loop) antenna and a mu-negative (MNG) shell (by duality), as well as for either an electric or magnetic dipole with a DNG shell. If one assumes that the permittivity and permeability of a medium are dispersive and the overall medium has no absorption, the time average of the total electromagnetic field energy is given by the well-known expression [12]

$$W_{\mathrm{total}}^{\mathrm{dispersive}} = \int\int\int_V \mathrm{d}V \left[\frac{1}{4} \{\partial_\omega[\omega\varepsilon_r(\omega)]\} \varepsilon_0 |\vec{E}_\omega(\vec{r})|^2 + \frac{1}{4} \{\partial_\omega[\omega\mu_r(\omega)]\} \mu_0 |\vec{H}_\omega(\vec{r})|^2 \right] \tag{10}$$

where $\vec{E}_\omega(\vec{r})$ and $\vec{H}_\omega(\vec{r})$ represent the time harmonic fields at the angular frequency ω. With the permeability being assumed to be non-dispersive (frequency independent) and equal to the free space value throughout this discussion, that is, $\mu_r(\omega) = 1$, (10) reduces immediately to the expression

$$W_{\mathrm{total}}^{\mathrm{dispersive}} = \int\int\int_V \mathrm{d}V \left[\frac{1}{4} \{\partial_\omega[\omega\varepsilon_r(\omega)]\} \varepsilon_0 |\vec{E}_\omega(\vec{r})|^2 + \frac{1}{4} \mu_0 |\vec{H}_\omega(\vec{r})|^2 \right] \tag{11}$$

We re-iterate that this expression is derived under the assumption that the medium is mainly transparent, that is, that there is no absorption. Thus in our discussion we will concentrate on the lossless dispersion models that result from various constraints on the field energy.

In the work of Landau and Lifshitz [12], the following general constraints are noted for the derivatives of the relative permittivity

$$\begin{aligned} &\partial_\omega(\varepsilon_r) \geq 0 \quad \text{passive material} \\ &\partial_\omega(\omega\varepsilon_r) \geq 0 \quad \text{positive definite energy} \\ &\partial_\omega(\omega\varepsilon_r) \geq 1 \quad \text{greater than or equal to the free space value} \end{aligned} \tag{12}$$

Clearly, a non-dispersive case, that is, $\partial_\omega(\varepsilon_r) = 0$, recovers the lower bound of the first constraint. On the other hand, the third condition (i.e. the free space value $\partial_\omega(\omega\varepsilon_0) = \varepsilon_0$) is the most stringent of these Landau–Lifshitz (LL) criteria. Thus, one can argue that an ENG metamaterial, which must be physically dispersive, has the following lower bound on the frequency behaviour of its relative permittivity

$$\partial_\omega(\omega\varepsilon_r) = \varepsilon_r + \omega\partial_\omega(\varepsilon_r) = 1 \quad \text{LL limit} \tag{13}$$

It is labelled as the 'LL limit' for comparison purposes. It is noted that the third condition arises from the direct sum of the first condition [Eq. 64.1, 12] written in the form: $\omega\partial_\omega[\varepsilon_r(\omega)] \geq 0$, and yet another derived condition [Eq. 64.2, 12]: $\omega\partial_\omega[\varepsilon_r(\omega)] \geq 2[1 - \varepsilon_r(\omega)]$. It can also be interpreted as the requirement that the difference between the fields in the medium and the same fields in vacuum be positive definite, that is, $W_{\mathrm{total}}^{\mathrm{dispersive}} - W_{\mathrm{total}}^{\mathrm{non\text{-}dispersive}} \geq 0$. This LL limit is the one assumed in the work of Smith and Kroll [13] and Tretyakov [14].

Unfortunately, this does not completely resolve the issue at hand. An ENG metamaterial is not a transparent medium; only evanescent waves can exist within an ENG layer. Consequently, the LL result may not be the most appropriate one for our metamaterial-based antenna systems. For instance [7], the condition $W_{\mathrm{total}}^{\mathrm{dispersive}} - W_{\mathrm{total}}^{\mathrm{non\text{-}dispersive}} \geq 0$ is also considered and a different condition is reported. In particular, the constraint is a different combination of the LL results: $\omega\partial_\omega[\varepsilon_r(\omega)] \geq 2[1 - \varepsilon_r(\omega)] \geq 0$. The limiting condition thus becomes

$$\varepsilon_r + \frac{1}{2}\omega\partial_\omega(\varepsilon_r) = 1 \quad \text{YB limit} \tag{14}$$

It is found immediately that the Drude model satisfies this limit, that is, $\omega\partial_\omega\varepsilon_{r,\mathrm{Drude}} = 2(\omega_{\mathrm{p}}/\omega)^2$, so that $\varepsilon_{r,\mathrm{Drude}} + 0.5\omega\partial_\omega\varepsilon_{r,\mathrm{Drude}} = 1$. The YB result thus says that one can do no better than a Drude model for passive dispersive media. Below, we will simply refer to the Drude dispersion model for this limit.

As discussed by Milonni [15], the constraint on the metamaterials with negative behaviours is obtained simply by requiring that the overall electric and magnetic field energies be independently positive definite, that is, $W_{\mathrm{electric}}^{\mathrm{dispersive}} \geq 0$ and $W_{\mathrm{magnetic}}^{\mathrm{dispersive}} \geq 0$. In our case this means $\partial_\omega(\omega\varepsilon_r) \geq 0$, which is a more relaxed condition than either the YB or LL limits. This constraint is used in the work of Caloz and Itoh [16] and Scalora *et al.* [17]; it is called the entropy condition [16]. The lower bound of this constraint is

$$\partial_\omega(\omega\varepsilon_r) = \varepsilon_r + \omega\partial_\omega(\varepsilon_r) = 0 \quad \text{M limit} \tag{15}$$

It is labelled as the 'M limit' for comparison purposes.

Further consideration of Poynting's theorem, which describes the electromagnetic power flow into and out of a region of space, suggests that the energy constraint only be that the total energy be positive definite. Because the magnetic energy will necessarily be positive in the cases we are considering, this means that we can rewrite the condition that $W_{\text{total}}^{\text{dispersive}} \geq 0$ as

$$\iiint_V \mathrm{d}V\left[\frac{1}{4}\partial_\omega(\omega\varepsilon_r)\varepsilon_0\left|\vec{E}(\vec{r})\right|^2\right] \geq -\iiint_V \mathrm{d}V\left[\frac{1}{4}\mu_0\left|\vec{H}(\vec{r})\right|^2\right] \quad (16)$$

If one assumes that the metamaterial and its dispersion properties are spatially homogeneous throughout the volume it occupies, then one can rewrite this relation as

$$\partial_\omega(\omega\varepsilon_r) \geq \frac{-\iiint_V \mathrm{d}V\left[\mu_0\left|\vec{H}\right|^2\right]}{\iiint_V \mathrm{d}V\left[\varepsilon_0\left|\vec{E}\right|^2\right]} \simeq -\left|\frac{Z_0}{Z_{\text{eff}}}\right|^2 \quad (17)$$

where Z_{eff} is the effective wave impedance in that region. If the fields are being resonantly propagated through that volume, one would expect that at the resonant frequency $Z_{\text{eff}} \simeq Z_0$. Consequently for an ENG layer in the resonant systems under consideration below, this means the behaviour of the dispersion should satisfy $\partial_\omega(\omega\varepsilon_r) \geq -1$. The corresponding lower limit is thus the smallest rate of change considered here. It is labelled as the 'Z limit' for comparison purposes and is given by the expression

$$\partial_\omega(\omega\varepsilon_r) = \varepsilon_r + \omega\partial_\omega(\varepsilon_r) = -1 \quad \text{Z limit} \quad (18)$$

This Z limit is the least restrictive constraint.

The lower bounds of the LL, M and Z constraints may be summarised with the equation

$$\partial_\omega(\omega\varepsilon_r) = c \quad (19)$$

where, respectively, the constant $c = +1, 0, -1$. A general dispersion model is derived straightforwardly that recovers these lower bounds at the frequency of interest f_0 and that satisfies the standard high-frequency limit

$$\lim_{\omega\to\infty} \varepsilon_r(\omega) = 1 \quad (20)$$

It has the form

$$\varepsilon_r(\omega) = 1 - a\left(\frac{\omega_0}{\omega}\right)^b \quad (21)$$

where

$$a = 1 - \varepsilon_r(\omega_0) \quad (22)$$

$$b = 1 + \frac{c-1}{a} \quad (23)$$

Given an interval surrounding the frequency of interest, $[f_0 - \Delta f, f_0 + \Delta f]$, the choice that $\partial_f(f\varepsilon_r)(f_0) = c$ rather than $\partial_f(f\varepsilon_r)(f_0 - \Delta f) = c$ means that (19) will be violated over the lower half of that interval. Nonetheless, the numerical convenience of using (21) as the dispersion model over a specified frequency interval centred at f_0 is significant. As confirmed by simulation, the errors introduced with the former choice are negligible because the frequency bandwidths of interest are so small when ka is small and the rate of change specified by (21) is thus small for each of the three cases.

3 Infinitely small dipole-multilayered spherical metamaterial shell systems: analytical results that include an ENG layer

The geometry of the multilayered electrically small dipole-metamaterial shell system is given in Fig. 1. The nested concentric spherical shells were constructed using N consecutive, homogeneous and isotropic metamaterial spheres with monotonically increasing radius values. The infinitesimal electrical dipole antenna is positioned at the centre of these shells and is oriented in the z-direction. The outer radius of the Nth sphere is r_N. Region M is the volume between the $(N-1)$th sphere and the Nth sphere and has the material parameters ε_M, μ_M where $M = 1, 2, \ldots, N$ and the 0th sphere is assumed to have a zero volume. The total power radiated through a sphere far from this dipole-metamaterial shell system is desired.

The analytical solution to this problem is a straightforward generalisation of the dipole-single metamaterial shell system problem [9–11]. In its full generality, the antenna-metamaterial multilayered shell system performance can be tested using layers consisting of any of the four possible media choices, for example, double-positive (DPS), epsilon-negative (ENG), mu-negative (MNG) and double-negative (DNG). We will emphasise a multilayered shell system consisting of a total of five regions below; in particular, one ENG layer and four DPS regions. The performance of the antenna-multilayered shell system can only be truly characterised by analysing many of the system variables simultaneously. As a natural consequence, it requires a more robust analysis method than simple brute-force trials to realise the optimum sphere dimensions and/or material parameters that will generate the maximum far-field radiated power. An optimisation model based upon the MATLAB® optimisation toolbox was successfully integrated with the system of equations describing the infinitesimal dipole-multilayered metamaterial shell system problem to optimise the total far-field radiated power. The constrained minimisation function, fmincon, was used to find the constraint minimum of a scalar function of many variables starting with an initial estimate. In particular, the optimisation variables were randomly initialised and the optimisation routines were supplied with a function $-f$, where f is the function being minimised. All of the radii and material parameters were encompassed in this minimisation function. Possible values for each design parameter were then supplied to the optimisation model. For instance, if the relative permittivity of one region was optimised, then an interval of possible values, for example, between $\varepsilon_r = -1$ and $\varepsilon_r = -20$, were supplied to the optimiser. A global optimisation value was finally obtained to produce the maximised far-field radiated power. This optimised

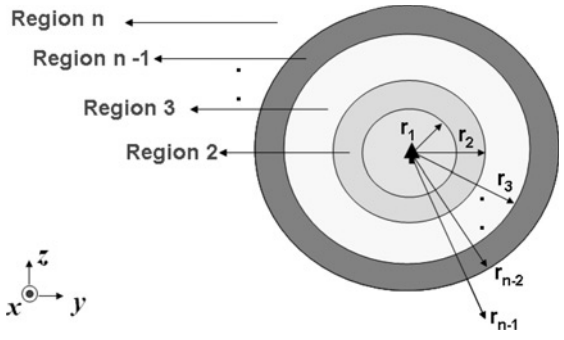

Fig. 1 *Geometry of the infinitely small electric dipole-multilayer metamaterial shell system*

analytical–numerical solution approach was validated with a variety of three-region problems corresponding to the cases reported in the work of Ziolkowski *et al.* [9–11]. In fact, we will first use these three-region (air–ENG–air) cases to discuss the dispersion limits.

3.1 Three-region antenna system with dispersion: passive metamaterials

To begin our considerations of the behaviour of the bandwidths associated with the various dispersion limit models, we first consider a three-region infinitesimal electric dipole–ENG spherical shell system similar to those given in the work of Ziolkowski *et al.* [11]. This allows us to connect those results with the multilayered systems presented below. The inner sphere, Region 1, and the outer region, Region 3, were both free space with ε_1, $\varepsilon_3 = \varepsilon_0$, where ε_0 is the free space permittivity value. The permittivity of the lossless ENG shell, Region 2, was first specified to be the frequency-independent value $\varepsilon_2 = -3\varepsilon_0$. The relative magnetic permeability of each region was assumed to be that of free space, that is, $\mu_1 = \mu_2 = \mu_3 = 1.0$. The length of the dipole was $l = 10\,\text{mm} = \lambda_0/100$. The radius of the inner sphere was taken to be 8.0 mm, that is, 60% larger than the assumed half-length of the antenna. We note that the inner sphere size, in theory, can be assigned to any value larger than the half-length of the dipole. However, when the tips of the antenna are very near to the inner surface of the ENG shell, they interact strongly. We avoid this situation since it may impact the performance of the overall antenna system. Moreover, the additional distance gives us some flexibility when we further optimise the system parameters to achieve complete matching. The outer radius of Region 2 was then optimised to define the resonant configuration. This was achieved by finding the outer radius that produced the maximum of the radiated power ratio (RPR)

$$\text{RPR} = 10\log_{10}\left[\frac{P_{\text{with shell}}(\text{1A input current})}{P_{\text{without shell}}(\text{1A input current})}\right](\text{dB}) \quad (24)$$

It is a parameter associated with the analytical model that enables us to quantify the total power radiated by an infinitesimal dipole-multilayered spherical shell system relative to the same infinitesimal dipole radiating in free space, both antennas being driven with the same idealised current value. The resonant dipole configuration was obtained with $r_{2,\max} = 14.9658$ mm. The Chu limit of the quality factor for this resonant configuration was thus $Q_{\text{Chu}} = 1213$. The corresponding fractional bandwidth is $\text{FBW}_{\text{Chu}} = 0.082\%$.

The various dispersion models were then incorporated into the isotropic and homogeneous ENG shell region. We note that for these cases $\varepsilon_{2r}(\omega_0) = -3.0$ and, hence, the dispersion models are

$$\begin{aligned}
\varepsilon_{2r,\text{Drude}}(\omega) &= 1 - 4\left(\frac{\omega_0}{\omega}\right)^2 \\
\varepsilon_{2r,\text{LL}}(\omega) &= 1 - 4\left(\frac{\omega_0}{\omega}\right) \\
\varepsilon_{2r,\text{M}}(\omega) &= 1 - 4\left(\frac{\omega_0}{\omega}\right)^{3/4} \\
\varepsilon_{2r,\text{Z}}(\omega) &= 1 - 4\left(\frac{\omega_0}{\omega}\right)^{1/2}
\end{aligned} \quad (25)$$

The RPR values as functions of the driving frequency were generated; several of these results are shown in Fig. 2. The fractional bandwidths were obtained from these RPR

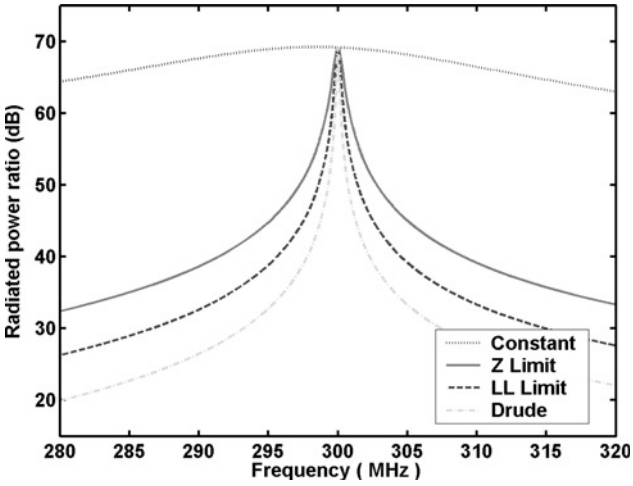

Fig. 2 *RPR for the resonant electric dipole–ENG spherical shell system with $r_1 = 8.0$ mm and $r_2 = 14.5968$ mm, the ENG metamaterial being described by several dispersion models with $\varepsilon_r(f_0) = -3.0$*

results. As shown in the work of Ziolkowski *et al.* [11], these analytical RPR-based fractional bandwidths slightly underestimate those obtained from the more realistic centre-fed dipole–ENG spherical shell numerical models. The corresponding Q values were $Q_{\text{Drude}} = 1.59Q_{\text{Chu}}$, $Q_{\text{LL}} = 0.800Q_{\text{Chu}}$, $Q_{\text{M}} = 0.603Q_{\text{Chu}}$ and $Q_{\text{Z}} = 0.405Q_{\text{Chu}}$. In particular, we note that all of the dispersion cases, but the Drude (YB) model, provided Q values below the Chu limit. We also note that the Drude and LL model results agree well with those obtained for the related resonant structure studied in the work of Ziolkowski *et al.* [11].

To examine this behaviour further, a comparison of the quality factors obtained for several different sizes of the proposed metamaterial-based antenna system with the limit-based dispersion models (24) and those obtained from the Chu limit expression was made. These results are summarised in Fig. 3. For this comparison, the inner radius of the ENG shell was fixed at $r_1 = 8.0$ mm and the outer radius was varied discretely from $r_2 = 12.0$ mm to $r_2 = 20.0$ mm with the ENG permittivity value $\varepsilon_{2r}(f_0)$ being optimised for each case to achieve the maximum resonant RPR value at or very near to $f_0 = 300$ MHz. These data are represented in Fig. 4 in terms of the ratio of the Q factors

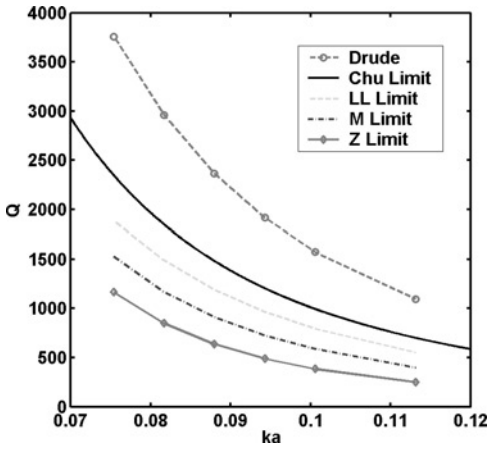

Fig. 3 *Comparison of the quality factors obtained for resonant electric dipole–ENG spherical shell systems with several different dispersion models of the passive ENG metamaterial and those obtained from the Chu limit as a function of the overall ka value*

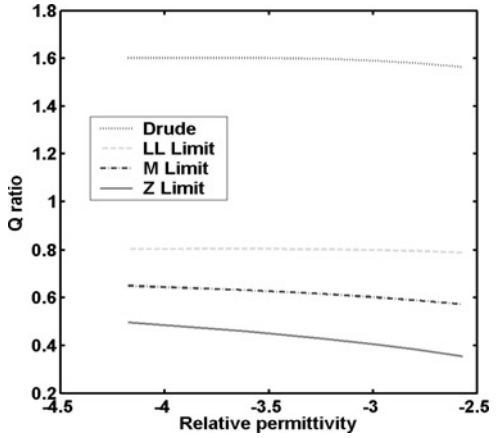

Fig. 4 *Comparison of the quality factors given in Fig. 3 normalised by the corresponding Chu limit value as a function of the relative permittivity of the ENG shell*

obtained for the dispersion limit model cases to the corresponding Chu values for those configurations against their optimised relative permittivity values. One also finds that as determined in the work of Ziolkowsik *et al.* [11], the required relative permittivity must become more negative as the shell thickness and, hence, the *ka* decreases to maintain the resonant configuration. It is clear from Figs. 3 and 4 that the theoretical quality factors associated with all of the dispersion limit models are below the Chu limit values, whereas the Drude model values are slightly above it for all of the resonant configurations. Although it will become more apparent in the resonant multilayered structures, Fig. 4 shows that the thicker the metamaterial shells are and, hence, the less negative the ENG metamaterial is, the Q factors are smaller and, thus, the improvement over the Chu limit increases.

3.2 Three-region antenna system: dispersion engineering with active metamaterials

Although most of the dispersion limit model metamaterial-based antenna systems discussed in the previous section outperform the traditional Chu limit system, the resulting useful bandwidth remains very small. On the other hand, from Fig. 2 one finds that the ideal non-dispersive metamaterial-based antenna system, being only $ka = 0.094$, has a remarkable $Q_{\text{ideal}} = 12.0345$ and, hence, $\text{FBW}_{\text{ideal}} = 8.309\%$. This system would be a very useful system.

The use of active circuit elements to achieve matched electrically small systems, the so-called non-Foster systems, has been considered, for instance, in the work of Skahill *et al.* [18]. Active systems are of potential interest because they are, in principle, not restricted by the Chu limit. Could one engineer the dispersion of the ENG shell in an active manner to recover the ideal fractional bandwidth associated with a non-dispersive metamaterial? To investigate this possibility, we have considered the ENG shell to be filled with an isotropic and homogeneous active metamaterial.

From the passive medium cases above, one recognises that one would want the frequency variation of the relative permittivity of the ENG medium to be as small as possible throughout the frequency interval of interest. We thus introduce a relative permittivity model created with two Lorentz resonances, one active (frequency above the operating frequency) and one passive (frequency below the operating frequency)

$$\varepsilon_{r,\text{Lorentz Gain}}(\omega) = 1 + \frac{\chi_{\text{passive}}\omega_{\text{p1}}^2}{-\omega^2 + j\omega\Gamma_1 + \omega_{00,1}^2} + \frac{\chi_{\text{active}}\omega_{\text{p2}}^2}{-\omega^2 + j\omega\Gamma_2 + \omega_{00,2}^2} \quad (26)$$

separated from each other sufficiently so that at the target frequency f_0 their combined values will have a very small slope. The use of gain media of this type to tailor the dispersion properties of slow and fast light systems (see [15, 19–21] for further discussions and references) and to achieve a negative refractive index medium [22] has been considered recently. To achieve the desired target frequency value of the relative permittivity: $\varepsilon_r(f_0) = -3.0$, we set the plasma frequencies $f_{\text{p1}} = f_{\text{p2}} = f_0$; the frequency of the passive resonance $f_{00,1} = 0.08f_0$ and its the coupling coefficient $\chi_{\text{passive}} = +1.2$; and the frequency of the active resonance $f_{00,2} = 1.78f_0$ and its coupling coefficient $\chi_{\text{active}} = -6.0548$. To maintain the lossless nature of the ENG medium, we set the collision frequencies $\Gamma_1 = \Gamma_2 = 0.0$. The RPR values resulting from modelling the ENG layer with this lossless Lorentz–Lorentz gain model is compared with the non-dispersive and the LL limit models in Fig. 5. The bandwidth for this active Lorentz–Lorentz gain medium is clearly much larger than the LL limit value. In particular, $\text{FBW}_{\text{Lorentz Gain}} = 3.647\% = 44.48\ \text{FBW}_{\text{Chu}}$ so that $Q_{\text{Lorentz Gain}} = 27.417 = 0.0226\ Q_{\text{Chu}}$.

In addition, because of the dispersion properties exhibited by several types of metamaterials realised to date, we also considered another gain medium in which the passive component was described by a two-time-derivative Lorentz material (2TDLM) model [23–26]. For instance, the dispersion properties of a split-ring resonator are described by a 2TDLM model. This model is desirable because the frequency behaviour above the resonance is flatter than that obtained from a Lorentz model. The resulting relative permittivity of this active 2TDLM–Lorentz medium is

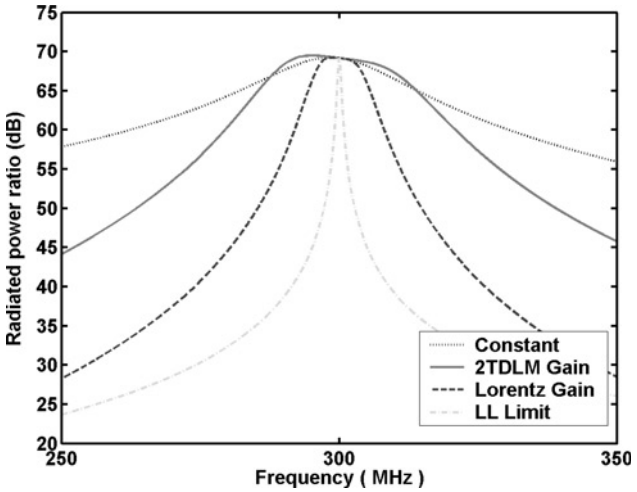

Fig. 5 *RPR for a $\ell = 10$ mm infinitesimal dipole in the presence of several optimised passive and active ENG spherical shells, all with relative permittivity value $\varepsilon_{r,ENG}(f_0) = -3.0$, and radii $r_1 = 8.0$ mm and $r_4 = 14.9658$ mm*

thus given by the expression

$$\varepsilon_{r,\mathrm{2TDLM\ Gain}}(\omega) = 1 + \frac{-\chi_{\mathrm{2TDLM}}\,\omega^2}{-\omega^2 + j\omega\Gamma_1 + \omega_{00,1}^2} + \frac{\chi_{\mathrm{Lorentz}}\,\omega_{\mathrm{p2}}^2}{-\omega^2 + j\omega\Gamma_2 + \omega_{00,2}^2} \quad (27)$$

To achieve the desired lossless model whose value of the relative permittivity at the target frequency is $\varepsilon_r(f_0) = -3.0$, we set the plasma frequencies $f_{\mathrm{p1}} = f_{\mathrm{p2}} = f_0$; the collision frequencies $\Gamma_1 = \Gamma_2 = 0.0$; the frequency of the passive 2TDLM resonance $f_{00,1} = 0.2492\,f_0$ and its coupling coefficient $\chi_{\mathrm{2TDLM}} = -2.9881$; and the frequency of the active Lorentz resonance $f_{00,2} = 2.112\,f_0$ and its coupling coefficient $\chi_{\mathrm{Lorentz}} = -2.8169$. The frequency separation between the resonances is larger than in the Lorentz–Lorentz gain case to take advantage of the ability of the 2TDLM–Lorentz model to achieve a larger frequency interval over which its slope is small. The RPR values resulting from incorporating this active 2TDLM–Lorentz medium into the ENG shell are also given in Fig. 5. The corresponding fractional bandwidth was $\mathrm{FBW}_{\mathrm{2TDLM\ Gain}} = 8.219\% = 100.23\ \mathrm{FBW}_{\mathrm{Chu}}$ so that $Q_{\mathrm{2TDLM\ Gain}} = 12.167 = 0.010\ Q_{\mathrm{Chu}}$. Thus, we have demonstrated that the introduction of an active ENG metamaterial into the electrically small resonant dipole–ENG spherical shell system allows one to achieve Q values of the same smallness as the nondispersive medium predictions. These Q values are significantly below the Chu limit and, hence, yield fractional bandwidths that are significantly larger than the Chu limit value. These bandwidth values are quite interesting for a variety of applications.

3.3 Finite element model of the three-region antenna system

It is recognised that it would be highly desirable to have overall efficiency and Q value results for the more realistic antenna systems such as the centre-fed dipoles or coax-fed monopoles surrounded by dispersive ENG shells. In particular, if the input impedances of these systems could be obtained, one could use the Yaghjian and Best result, [Eq. 87, 7], to calculate the quality factor as

$$Q_{\mathrm{YB}} = \frac{f_0}{2R_{\mathrm{input}}(f_0)}\left|(\partial_f Z_{\mathrm{input}})(f_0)\right| = \frac{f_0}{2R_{\mathrm{input}}(f_0)}\sqrt{[\partial_f R_{\mathrm{input}}(f_0)]^2 + [\partial_f X_{\mathrm{input}}(f_0)]^2} \quad (28)$$

However, to realise the less than 0.1% in bandwidth (which is the typical Chu result for the systems under consideration here) with a source wavelength at 1.0 m (300 MHz), for the dispersive medium shells, the discretisation required to achieve a complete three-dimensional (3D) HFSS simulation model is impractical. As will be discussed below, the frequency-independent ENG shell HFSS simulations use over 100 000 tetrahedra and simple scans in frequency take several days to complete. However, we have found that the COMSOL Multiphysics axi-symmetric two-dimensional (2D) simulator is ideally suited to the rotationally symmetric geometries considered above. By demonstrating that the analytical RPR-based approach with infinitesimal antennas provides reasonable answers to the dispersion issues in comparison to these numerical models with more realistic radiating elements, we will then use the idealised analytical models with confidence in their predictive capabilities for the more complicated and computationally demanding five-region systems.

The advantage provided by COMSOL Multphysics over HFSS ANSOFT for this dispersive ENG shell investigation is thus simply an issue of numerics, not physics. Being able to use 2D axi-symmetric geometries, we can use 130 000 unknowns in 2D rather than in 3D. This gives us more than an order of magnitude more resolution in the numerics, and hence allows us to consider the dispersive realistic geometries. In particular, we have been able to simulate the realistic coax-fed monopole–ENG hemispherical shell system with all of the dispersion models for the ENG shell.

The COMSOL Multiphysics simulation was first designed with the non-dispersive ENG shells to achieve the desired resonant system. In particular, an input impedance $Z_{\mathrm{input}} = 49.90 - 3.48 \times 10^{-4}\,\mathrm{j}\ \Omega$ was obtained at a resonance frequency of $f_{\mathrm{res}} = 299.99$ MHz for the 50 Ω source with the parameters: coax inner conductor radius $a = 1.2$ mm; coax outer conductor radius $b = 2.301 \times a = 2.7612$ mm; monopole length $\ell = 4.0823$ mm; and ENG shell inner radius $r_1 = 8$ mm and outer radius $r_2 = 15.502$ mm with $\varepsilon_r(f_{\mathrm{res}}) = -3.0$. The number of degrees of freedom solved was 147 035. This very fine resolution mesh allowed us to decrease the frequency resolution to 5×10^3 Hz. The predicted overall efficiency was 99.99%. These values give $ka = 0.0973$ and $Q_{\mathrm{Chu}} = 1094.6$ at the resonance frequency. The quality factor obtained from the predicted resistance and reactance curves with Yaghjian and Best's formula, (28) was $Q_{\mathrm{YB}} \simeq 12.02 = 0.011 Q_{\mathrm{Chu}}$, in very good agreement with the analytical results.

The dispersive ENG shells were then simulated with this COMSOL Multiphysics model. Because the permittivity value is identical by design for each model at the resonance frequency, the overall efficiency of the antenna system, even with dispersion being present, remains 99.99%. On the other hand, because the slope of the resistance and reactance curves will change with each dispersion model, the resulting Q values will be different for each of them. The predicted values of Q/Q_{Chu} using (28) for all of the passive cases are given in Table 1 and for the active cases in Table 2. The corresponding RPR-derived results from the analytical resonant infinitesimal dipole–ENG shell system with $r_2 = 14.9658$ mm are also given in Tables 1 and 2. The agreement between the analytical RPR-based results and the numerical input-impedance-based results is very good. As noted previously, all of the dispersion limit models, except the Drude (Yaghjian–Best) version, have Q values below the corresponding Chu limit value. As to which dispersion model is the most correct one, the majority of references favour the Milonni (entropy) condition, that is, positive-definiteness independently of both the electric and magnetic field energies. The design of metamaterials to achieve these various constraints is currently in progress. It is hoped that one could determine experimentally which model gives the ultimate physical limitation on the dispersion properties. Nonetheless, these numerical results

Table 1: COMSOL Multiphysics predicted values of Q/Q_{Chu} for the dispersion-limit models

	Drude	Landau–Lifschitz	Entropy	Z	Frequency independent
Analytical	1.59	0.80	0.60	0.41	0.010
50 Ω coax case	1.68	0.84	0.64	0.43	0.011

Table 2: COMSOL Multiphysics predicted values of Q/Q_{Chu} for the gain medium dispersion models

	Lorentz–Lorentz gain medium	Lorentz–2TDLM gain medium
Analytical	0.023	0.010
50 Ω coax case	0.019	0.012

give us confidence that the analytically predicted Q values for the idealised antenna systems and, hence, their bandwidths are a very good indicator of the performance of the corresponding more realistic systems.

4 Dipole–(glass–ENG medium–glass) antenna system

We consider now the multilayered spherical structure; it will consist of five regions in this discussion. The five-region problem represents a configuration which could lead to a possible realisation of both the passive and active versions of the dipole–ENG spherical shell system. In particular, we consider a cold plasma realisation of the ENG region, that is, with Regions 2 and 4 being glass, we fill Region 3 with a cold plasma, which is described by the Drude dispersion model. This geometry is depicted in Fig. 6.

For a plasma density of N_e electrons per cm^3, the plasma frequency

$$f_p = \frac{\omega_p}{2\pi} = 8.98 \times 10^3 \sqrt{N_e} \tag{29}$$

Thus the plasma density required to produce a specific relative permittivity at the target frequency for the lossless model (9) is

$$N_e = 3.1437 \times 10^{-10}[1 - \varepsilon_{r,\text{real}}(\omega_0)]\omega_0^2 \tag{30}$$

Since the plasma in a typical fluorescent light tube has an electron density on the order of $10^{10} - 10^{11}$ cm^{-3}, one could use a plasma whose density $N_{e,res} = 1.229 \times 10^{+10}$ cm^{-3} to obtain the relative permittivity value $\varepsilon_{r,\text{real}}(\omega_0) = -10.0$. In particular, by filling the spherical glass bottle with a gas having $N_{e,res}$ atoms and arranging for a breakdown mechanism of this gas, the multilayer plasma (ENG) shell system could be realised. Since it may be experimentally attainable, we will use this relative permittivity value in the discussions below.

We note that, as shown in the work of Ziolkowski *et al.* [11], the corresponding coax-fed monopole in a multilayer plasma (ENG) hemi-spherical shell system would have essentially the same behaviour as the centre-fed cylindrical electric dipole-multilayer plasma (ENG) spherical shell system. The monopole-hemispherical glass–plasma–glass geometry may be the most straightforward approach to a proof-of-concept realisation of this system. Nonetheless, to be complete we have investigated both the spherical and hemispherical systems to determine their naturally resonant configurations.

4.1 Analytical modelling: frequency-independent ENG layer

The inner sphere, Region 1, and the outer region, Region 5, are assumed to be free space with $\varepsilon_1, \varepsilon_5 = \varepsilon_0$ where ε_0 is the free space permittivity value. The radius of Region 1 was again taken to be $r_1 = 8.0$ mm. The relative permittivity of the glass Regions 2 and 4 was assumed to be ε_2, $\varepsilon_4 = 2.25\varepsilon_0$. The thickness of these glass shells was fixed at 1.0 mm (as recommended by our University's fabrication facility for potential future experiments). Region 3 was taken to be the ENG medium with a relative permittivity ε_3. The relative magnetic permeabilities of the antenna system were assumed to be that of free space, that is, $\mu_1 = \mu_2 = \mu_3 = \mu_4 = \mu_5 = 1.0$. The total length of the infinitesimal dipole antenna was again assumed to be $\ell = 10.0$ mm $= \lambda_0/100$.

The relative permittivity of the ENG medium, Region 3, was first assumed to be homogeneous and frequency independent with a value $\varepsilon_r = -10$. The thickness of the ENG layer was then optimized to produce the maximum RPR. The final optimisation scenario was: $r_1 = 8.0$ mm, $r_2 = 9.0$ mm, $r_3 =$ (optimisation value -1 mm) and $r_4 =$ (optimisation value). The optimisation interval was constrained between $r_4 = 10$ mm and $r_4 = 20$ mm. The optimised r_4 value that produced the maximum RPR was $r_4 = 11.92656$ mm. The RPR value for this optimised configuration at the target frequency of 300 MHz was 74.594 dB. Reducing the shell thickness to a slightly more realisable value: $r_4 = 11.926$ mm, the RPR = 70.89 dB at 300 MHz. The RPR response as a function of frequency is shown in Fig. 7 for these system

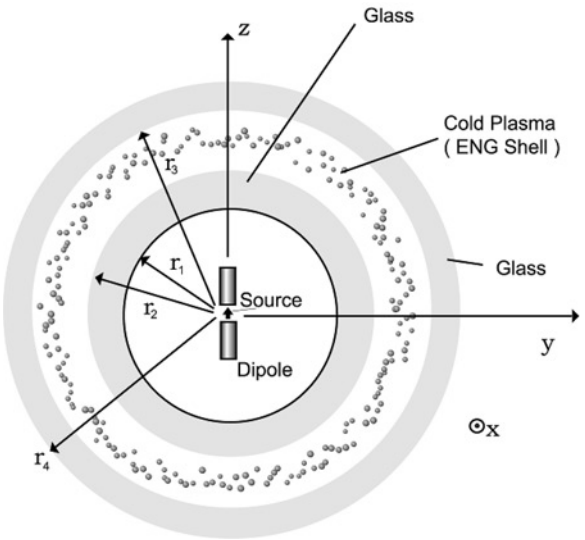

Fig. 6 *Geometry of the HFSS centre-fed cylindrical electric dipole-multilayer plasma (ENG) spherical shell system*

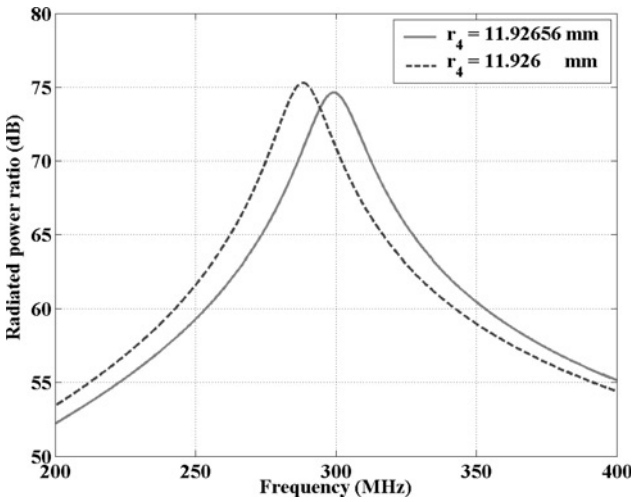

Fig. 7 *Total radiated power for a $\ell = 10$ mm infinitesimal dipole in the presence of an optimised glass–ENG–glass shell system normalised by the total power radiated by the same antenna in free space*

parameters: $r_1 = 8.0$ mm, $r_2 = 9.0$ mm, $r_3 = 10.926$ mm (10.92656 mm), $r_4 = 11.926$ mm (11.92656 mm) and $\varepsilon_3 = -10.0$. The resonant behaviour of this system is observed immediately. The magnitudes of the real part of the total electric and magnetic field distributions for the resonant lossless ENG spherical shell case with $r_4 = 11.92656$ mm are shown, respectively, in Fig. 8*a* and *b*. A comparison with these resonant field distributions with those given in the work of Ziolkowski *et al.* [11] convinces one that the resonant modes of this five-region case are only slight variations of those associated with the corresponding three-region case. We note that the optimisation routine produces a very precise value for the radius that achieves resonance at 300 MHz. Any rounding off of this value impacts the overall performance of the resonant system. One would simply have to adjust the material properties and radii to retune the system for these less precise values.

The infinitesimal dipole-multilayered ENG spherical shell system has the fractional bandwidth $\text{FBW}_{\text{Analytical}} = 6.26\%$ and the quality factor $Q_{\text{Analytical}} = 15.964$. The corresponding Chu limit values with $k_0 r_{4,\ \text{optimized}} = 0.074936$ are $Q_{\text{Chu}} = 2389.71$ and $\text{FBW}_{\text{Chu}} = 0.042\%$. Consequently, this idealised case provides a quality factor significantly below the Chu value: $Q_{\text{Analytical}} = 0.0067\ Q_{\text{Chu}}$. We note, however, that the ideal value for this configuration is slightly above the $\varepsilon_3 = -3.0$ value discussed in the previous section. This occurs because of the introduction of the additional interfaces. The system simply has less bandwidth because it is more sensitive, having had to achieve matching across four interfaces instead of two.

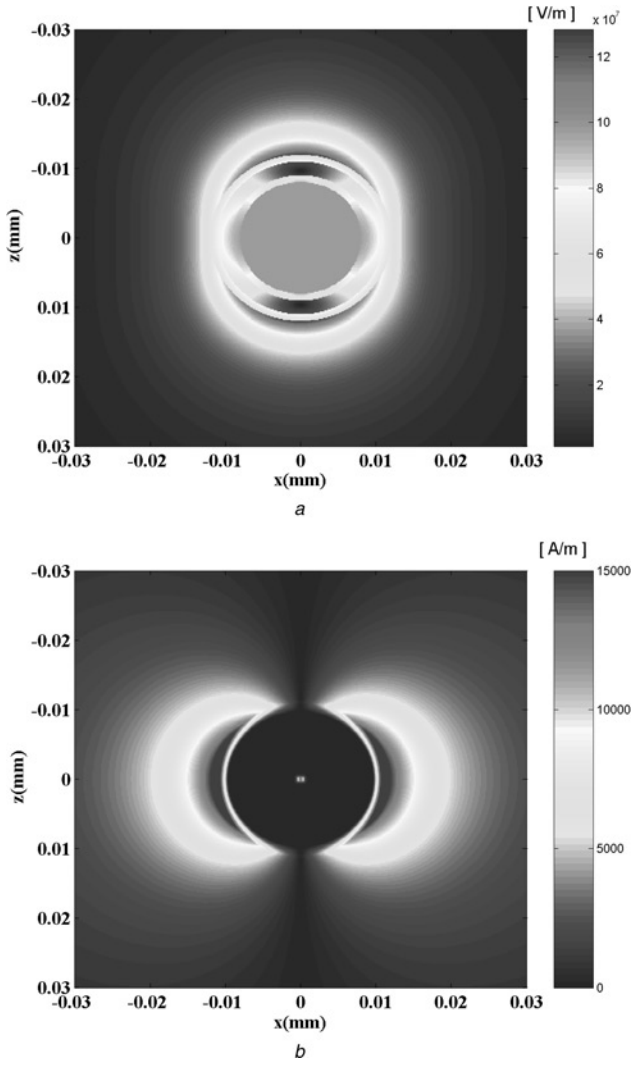

Fig. 8 *Electric (a) and magnetic field (b) distributions for a $\ell = 10$ mm infinitesimal dipole radiating in the presence of the optimised glass–ENG–glass spherical shell system*

a E-field distribution
b H-field distribution

4.2 HFSS numerical modelling: frequency-independent ENG layer

To compare the analytical infinitesimal dipole results with a more realistic centre-fed dipole, a 300 MHz thin cylindrical dipole antenna of length $\ell = 10$ mm that had a lumped element feed was modelled with HFSS in the presence of the same glass–ENG–glass spherical shell system. The radius of the cylindrical dipole antenna was $r_{\text{antenna}} = 0.1\ \text{mm} = \lambda_0/1000$ so that the aspect ratio $\ell/(2r_{\text{antenna}}) = 50.0$. The resistance and reactance values of the lumped element source were set to 75 Ω and 0 Ω, respectively. We calculated the total radiated power of the antenna radiating into free space and radiating in the presence of the multilayered ENG spherical shell system when both antennas are driven with the same 1 W input power from the 75 Ω source. This allows us to introduce and use the relative gain (RG) parameter [8]

$$\text{RG} = 10\log_{10}\left[\frac{P_{\text{with shell}}(1\text{W input})}{P_{\text{without shell}}(1\text{W input})}\right](\text{dB}) \qquad (31)$$

to characterise the performance of the center-fed dipole multilayered ENG spherical shell system. Since we know the input power and the output power, the overall efficiency is readily obtained. Moreover, since we can calculate the input impedance as a function of the driving frequency, we can also calculate the Q and the bandwidth of this system.

The HFSS RG and the analytical RPR values were in very good agreement, particularly in the location of the resonance, its width and its peak value. The FBW obtained from the half-power points of the RG results was $\text{FBW}_{\text{RG}} = 8.54\%$ and, hence, the quality factor $Q = 11.70$. We note that the free space $\ell = 10$ mm dipole attached to a 75 Ω feedline radiated only 6.5356×10^{-8} W. Consequently, with no attempt to match the centre-fed dipole-multilayer ENG spherical shell system to the 75 Ω feedline, it radiated 0.5232 W, giving an overall efficiency equal to 52.32%. As extensively discussed in the work of Ziolkowski *et al.* [11], the dipole and the ENG spherical shell system can now be modified slightly to produce a complex conjugate reactance match and a resistance match to the source.

A resonant centre-fed cylindrical dipole-multilayered ENG spherical shell system that produced approximately a 75 Ω resistance and zero reactance near 300 MHz was then designed with a series of HFSS simulations. The detailed specifications of the HFSS model that was matched to the 75 Ω feedline are given in Table 3. Fig. 9 shows the HFSS predicted values of the complex input impedance values for the matched dipole-multilayered ENG spherical shell system as a function of the frequency. The zero crossing of the reactance (the antenna resonance frequency) occurs at 307.22 MHz and the resistance value at this frequency is 72.159 Ω. The resistance and reactance values at 300 MHz were 68.42 Ω and −53.43 Ω, respectively. The overall efficiency of this system for a 75 Ω source was found to be 87.62% at 300 MHz and 99.96% at 307.22 MHz. Fig. 10 demonstrates the potential overall efficiency and the corresponding S_{11} reflection coefficient values as a function of the frequency for both the original

Table 3: Detail specifications of the matched resonant dipole-multilayered ENG spherical shell system

Antenna length, mm	8.2
Antenna radius, mm	0.59
Gap length, mm	0.2
Gap radius, mm	0.59
Operation frequency, MHz	300
Lumped port resistance value, Ω	75
Lumped port reactance value, Ω	0
Shell radius (r_1), mm	8
Shell radius (r_2), mm	9
Shell radius (r_3), mm	10.928
Shell radius (r_4), mm	11.928

75 Ω source and for a 72.159 Ω matched source. Note that because of computational memory and time limitations, it was not possible to obtain a continuous plot of the overall efficiency and S_{11} reflection coefficient values from HFSS. Thus, we applied a third-order polynomial fit to the HFSS generated discrete impedance values within the frequency band between 275 MHz and 325 MHz to obtain the curves shown in Fig. 10.

Having the input impedance, we were able to calculate the bandwidth of the resonant centre-fed cylindrical dipole–(glass–ENG–glass) spherical shell system. The −3 dB frequency points of the overall efficiency (50% values) for the 75 Ω match in Fig. 10 are 288.32 MHz and 328.77 MHz. Consequently, the fractional half-power VSWR bandwidth [7] was $\text{FBW}_{\text{VSWR}} = 13.16\%$ and the corresponding quality factor, using (28), was $Q_{\text{VSWR}}(\omega_0) = 2/\text{FBW}_{\text{VSWR}}(\omega_0) = 15.19$. The derivative values of the resistance and reactance curves in Fig. 9 were also used to calculate (28), giving $Q_{\text{YB}} \simeq 15.53$. This value gives the so-called fractional conductance bandwidth $\text{FBW}_{\text{CD}} = 1/Q_{\text{YB}} = 6.44\%$, which, as pointed out by (42) of Yaghian and Best [7], is approximately half of the half-power VSWR fractional bandwidth value.

We note that all of these Q and FBW values are in very good correspondence among themselves. Moreover, we find that the bandwidth obtained from the analytical RPR values and, hence, that Q value is in very good agreement with the fractional conductance bandwidth and the Q values obtained from the VSWR and conductance bandwidths. We also note that all of these Q values are slightly smaller than the value predicted by the analytical model. We further emphasise that these Q values are significantly below the Chu limit because the ENG medium was assumed to be ideal, that is, frequency independent.

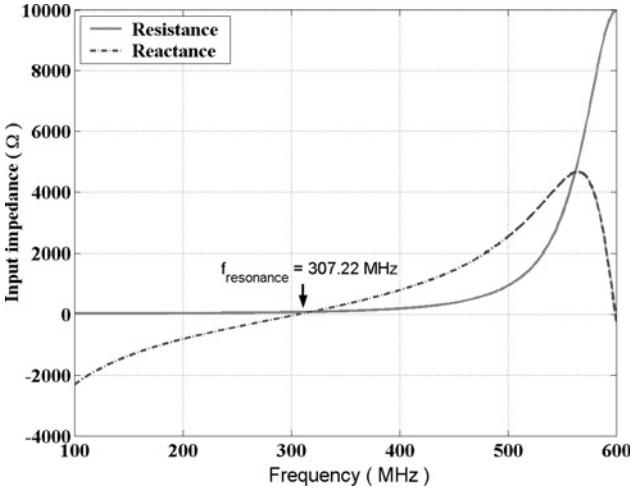

Fig. 9 *Complex-valued input impedance for the resonant centre-fed cylindrical dipole–(glass–ENG–glass) spherical shell system*

This system is conjugately matched (zero reactance) and resistance matched at 307.22 MHz to a 75 Ω feedline

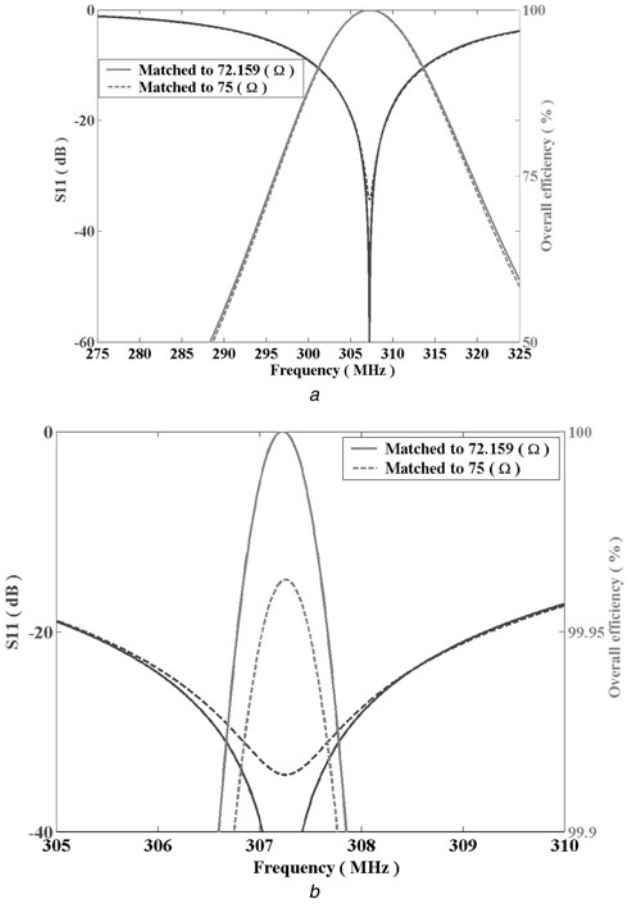

Fig. 10 *S_{11} and overall efficiency values against frequency for the resonant centre-fed cylindrical dipole–(glass–ENG–glass) spherical shell system*

a S_{11} and overall efficiency values
b Zoom
The curves for matching the dipole–ENG shell system to both 75 Ω and 72.159 Ω sources are given

Fig. 11*a* and *b* shows, respectively, plots of the HFSS predicted E- and H-field distributions at 300 MHz for the resonant centre-fed cylindrical dipole–(glass–ENG–glass) spherical shell system. These distributions are in very good agreement with the analytical results shown in Fig. 8*a* and *b*. The differences are a result of the presence of the centre-fed cylindrical dipole. Fig. 11*a* and *b* reveals the presence of large fields in the gap regions and near the ends of the dipole. Fig. 12 shows the corresponding HFSS predicted E- and H-plane patterns in the far-field region. The radiation patterns for both cases agree with the well-known dipole antenna radiation patterns confirming there is no variation in the pattern, hence the directivity, when the resonance occurs although there is an enhancement of the overall efficiency due to the presence of the matched multilayered ENG spherical shell system.

4.3 Analytical modelling: frequency-dependent ENG layer

As with the three-region problem, the dispersion models are readily included in the analytical solution of the five-region

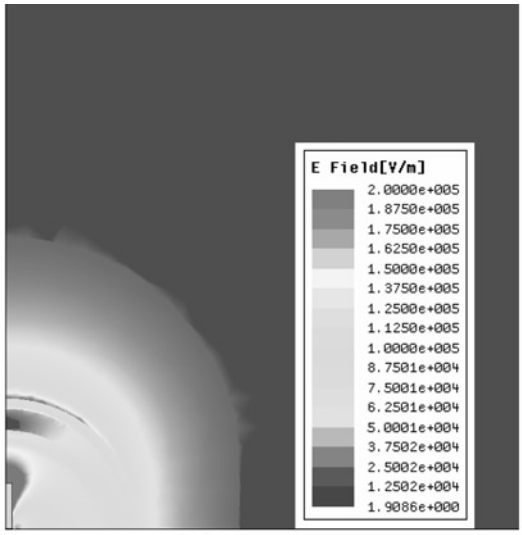

a

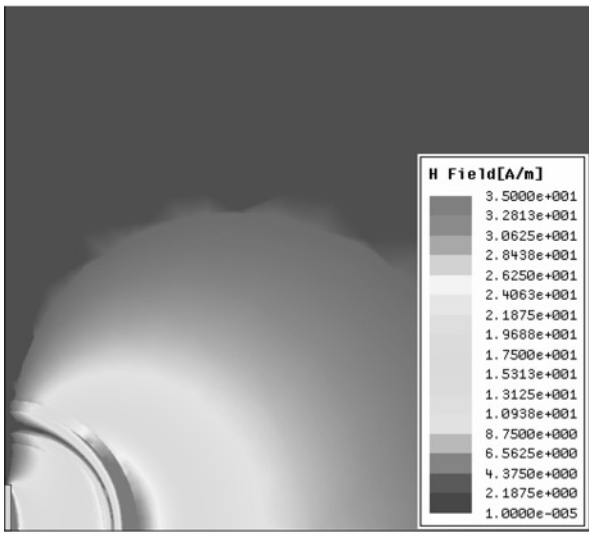

b

Fig. 11 *Distribution plots (in one quadrant) for the resonant centre-fed cylindrical dipole–(glass–ENG–glass) shell system at 300 MHz*

a E-field distribution
b H-field dictribution

multilayer problem. As in the work of Ziolkowski *et al.* [11], we have shown that the analytical and numerical models based upon the frequency-independent ENG medium predict essentially the same Q and FBW values. As a consequence and because of the extreme difficulty to achieve the requisite frequency and material property resolutions within the HFSS numerical solution, we have again focused on using the analytical model to analyse the effects of dispersion on the infinitesimal dipole–(glass–ENG–glass) spherical shell system.

The inner radius of the ENG shell was fixed at $r_1 = 8.0$ mm and the outer radius was again varied discretely from $r_2 = 12.0$ mm to $r_2 = 20.0$ mm with the value $\varepsilon_r(f_0)$ being optimised for each case to achieve the maximum resonant RPR value at $f_0 = 300$ MHz. Thus, the thickness of the ENG layer was varied from 2.0 mm to 10.0 mm. The resulting quality factors as functions of the overall ka values are shown in Fig. 13. As noted above, one finds that the five-region, four-interface spherical configurations are even more sensitive to the presence of dispersion than the three-region, two-interface configurations are. In particular, only the systems with the M and

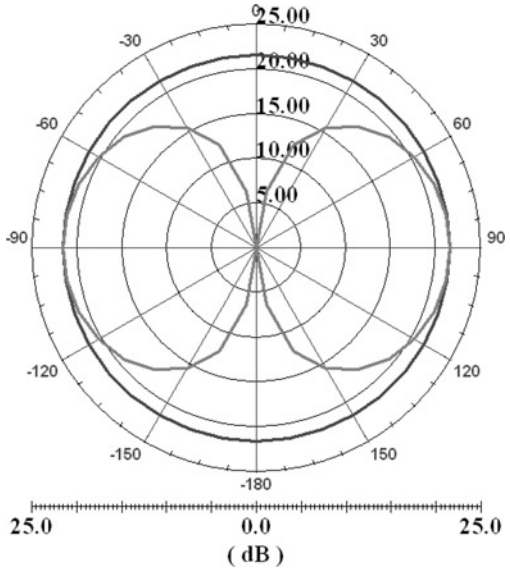

Fig. 12 *HFSS predicted E- and H-plane patterns in the far-field region for the resonant centre-fed cylindrical dipole–(glass–ENG–glass) shell system at 300 MHz*

The E-plane (H-plane) pattern is the grey (black) curve

Z limit models have quality factors below the Chu limit for most of the resonant configurations considered. The LL case results closely follow the Chu limit values. By normalising the quality factors by the corresponding Chu limit values and plotting these ratios as a function of the relative permittivity in the ENG layer in Fig. 14, one observes that the quality factors are further below the Chu limit when the ENG layer is thicker and has the largest relative permittivity. The cases with the largest relative permittivities provided quality factors further below the Chu limit. However, because the maintenance of very low plasma densities is challenging, there would be an eventual trade-off between the desired plasma density and, hence, the achievable quality factor in any experimental realisation of the centre-fed dipole–(glass–ENG–glass) system. On the other hand, the utilisation of the breakdown of an excited gas, as is done to produce the gain media in the slow–fast light studies [15, 19–21], affords us the opportunity to achieve a plasma that realises an active ENG medium.

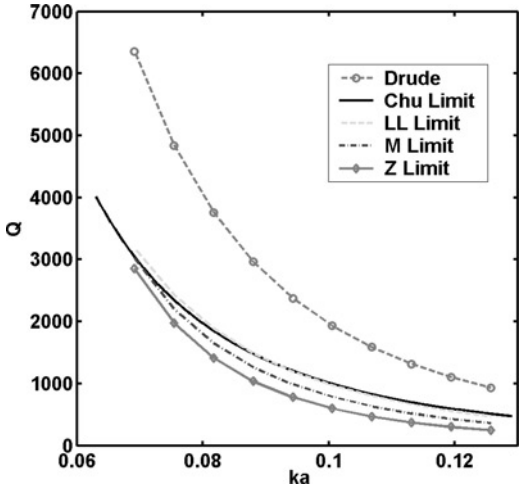

Fig. 13 *Comparison of the quality factors obtained for resonant glass–ENG–glass spherical shell systems with several different dispersion models of the passive ENG metamaterial and those obtained from the Chu limit, as functions of the ka of the ENG shell*

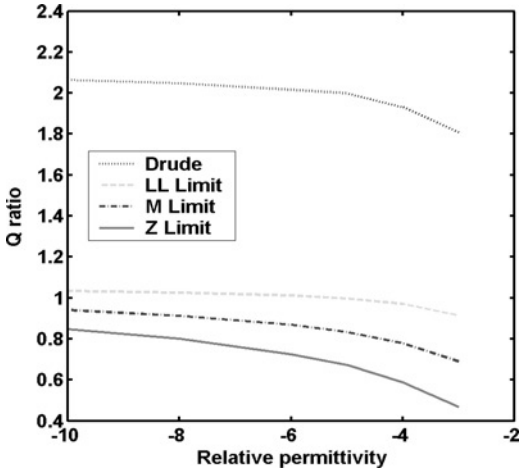

Fig. 14 *Comparison of the quality factors given in Fig. 13 normalised by the corresponding Chu limit value as a function of the relative permittivity of the ENG shell*

The RPR values obtained for the infinitesimal dipole–(glass–ENG–glass) spherical shell system with $r_1 = 8.0$ mm, $r_4 = 11.92656$ mm and $\varepsilon_r(f_0) = -10.0$ when the lossless ENG medium is assumed to be frequency independent and when it is described as an LL limit medium, as a Lorentz–Lorentz gain medium and as a 2TDLM–Lorentz gain medium are shown in Fig. 15. The Lorentz–Lorentz gain medium was obtained with the parameters: $f_{p1} = f_{p2} = f_0$; $\Gamma_1 = \Gamma_2 = 0.0$; $\chi_{passive} = +2.20$ and $f_{00,1} = 0.10\, f_0$; and $f_{00,2} = 2.205 f_0$ and $\chi_{active} = -33.90$. The 2TDLM–Lorentz gain medium was obtained with the parameters: $f_{p1} = f_{p2} = f_0$; $\Gamma_1 = \Gamma_2 = 0.0$; $f_{00,1} = 0.20\, f_0$ and $\chi_{2TDLM} = -8.805$; and $f_{00,2} = 2.34\, f_0$ and $\chi_{Lorentz} = -8.182$. The fractional bandwidths and quality factors for the cases shown in Fig. 15 are: $FBW_{Const} = 6.218\% = 148.05\ FBW_{Chu}$ so that $Q_{Const} = 16.08 = 0.0067\ Q_{Chu}$; $FBW_{LL} = 0.040\% = 0.95\ FBW_{Chu}$ so that $Q_{LL} = 2500.04 = 1.05 Q_{Chu}$; $FBW_{Lorentz\ Gain} = 2.796\% = 66.57\ FBW_{Chu}$ so that $Q_{Lorentz\ Gain} = 35.768 = 0.015\ Q_{Chu}$; and $FBW_{2TDLM\ Gain} = 6.793\% = 161.74\ FBW_{Chu}$ so that $Q_{2TDLM\ Gain} = 14.72 = 0.0062\ Q_{Chu}$. The bandwidth enhancements provided by the use of an active ENG medium are clearly significant. In fact, the quality factor (fractional bandwidth) for the active 2TDLM–Lorentz gain medium is even slightly below (above) the frequency-independent ENG medium case. As with the

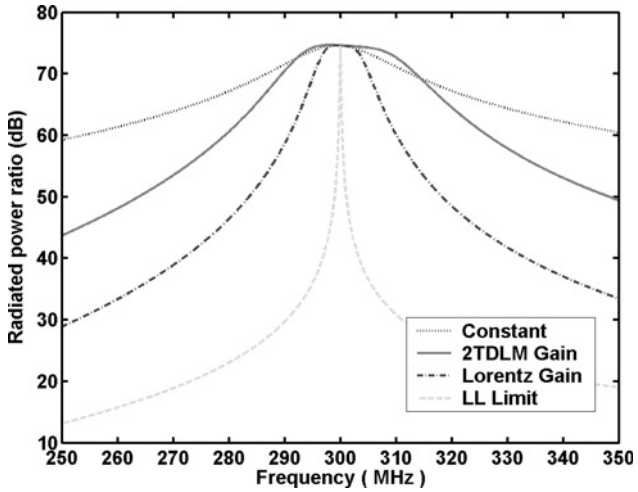

Fig. 15 *RPR for a $\ell = 10$ mm infinitesimal dipole in the presence of several optimised passive and active ENG glass–ENG–glass spherical shell systems, all with relative permittivity value $\varepsilon_{r,ENG}(f_0) = -3.0$, and radii $r_1 = 8.0$ mm and $r_4 = 11.92656$ mm*

dipole–ENG shell system, the introduction of an active metamaterial medium into the dipole–(glass–ENG–glass) shell systems leads to quality factors that are significantly below the Chu limit and, hence, to bandwidths of interest to a variety of applications.

We note that, in analogy to the results given in the work of Ziolkowski *et al.* [11], the corresponding coax-fed monopole in a glass–ENG–glass hemispherical shell system would have essentially the same behaviour as the centre-fed cylindrical electric dipole–(glass–ENG–glass) spherical shell system. The monopole–(glass–ENG–glass) hemispherical shell geometry may be the most straightforward approach to a proof-of-concept realisation of this system.

5 Conclusions

We have demonstrated theoretically that an efficient electrically small metamaterial-based antenna system whose quality factor (fractional bandwidth) is below (above) the Chu limit can be achieved. This antenna system is based upon surrounding an electrically small dipole antenna with a specifically designed electrically small, multilayered metamaterial spherical shell system that includes an ENG layer. It was shown with analytical and numerical results that this dipole-multilayered ENG spherical shell system can be designed to be resonant and impedance matched to a source; and, as a result, it can be an efficient radiator. It was demonstrated that the dispersion properties of the ENG layer have a significant impact only on the frequency bandwidth of the system and not its efficiency at the driving frequency. Several passive dispersion models were considered to examine the lower bound on the quality factor. A system based upon a passive dispersive ENG layer that produced a quality factor ~2.5 times below the Chu limit was demonstrated.

Because the non-dispersive ENG results exhibited even smaller Q values and, hence, larger bandwidths, we also considered the effects of active ENG media. It was demonstrated that by introducing an ENG medium with gain into the multilayered spherical shell system, one could realise a dipole-multilayered ENG spherical shell system that has a Q value that recovers the non-dispersive result, that is, a very small fraction of the Chu limit and, hence, exhibits a fractional bandwidth significantly larger (more than 2 orders of magnitude) than would be predicted by the Chu limit and that would be of interest to a variety of applications.

We are currently modelling other variants of the multilayered metamaterial spherical shell system. We are also planning a proof-of-concept experiment based upon the passive and active plasma models considered here to investigate the practical aspects of the dipole-multilayer ENG spherical shell system. It is very clear that very low loss and very low dispersion metamaterials will be necessary to achieve practical realisations of these systems. Because the field strengths will be very high near these electrically small systems, even low losses may still be too high for practical relevance or there may still be the usual trade-off between efficiency and bandwidth. With active materials one may be able to overcome even these loss issues. We have also begun investigating how to design low-loss active metamaterials that could be obtained with lumped element-based inclusions. We hope to report these results elsewhere in the near future.

6 Acknowledgments

The authors would like to thank several anonymous reviewers for their constructive comments which led to

important additions and changes to this paper. This work was supported in part by DARPA Contract Number HR0011-05-C-0068.

7 References

1 Chu, L.J.: 'Physical limitations of omnidirectional antennas', *J. Appl. Phys.*, 1948, **19**, pp. 1163–1175

2 Wheeler, H.A.: 'Fundamental limitations of small antennas', *IRE Proc., 1947*, **35**, pp. 1479–1484

3 Harrington, R.P.: 'Time harmonic electromagnetic fields' (McGraw-Hill, New York, 1961), pp. 414–420

4 Collin, R.E., and Rothschild, S.: 'Evaluation of Antenna Q', *IEEE Trans. Antennas Propag.*, 1964, **AP-12**, (1), pp. 23–27

5 Hansen, R.C.: 'Fundamental limitations in antennas', *Proc. IEEE*, 1981, **69**, pp. 170–181

6 McLean, J.S.: 'A re-examination of the fundamental limits on the radiation Q of electrically small antennas', *IEEE Trans. Antennas Propag.*, 1996, **AP-44**, pp. 672–676

7 Yaghjian, A.D., and Best, S.R.: 'Impedance, bandwidth, and Q of antennas', *IEEE Trans. Antennas Propag.*, 2005, **53**, (4), pp. 1298–1324

8 Balanis, C.A.: 'Antenna theory' (John Wiley & Sons, New York, 2005), pp. 637–641

9 Ziolkowski, R.W., and Kipple, A.: 'Application of double negative metamaterials to increase the power radiated by electrically small antennas', *IEEE Trans. Antennas Propag.*, 2003, **51**, pp. 2626–2640

10 Ziolkowski, R.W., and Erentok, A.: 'Dipole antennas enclosed in double negative (DNG) and single-negative (SNG) nested spheres: efficient electrically small antennas'. IEEE Antennas and Propagation Society International Symposium/URSI-USNC National Radio Science Meeting, Washington, DC, July 12–17 2005, 3–8

11 Ziolkowski, R.W., and Erentok, A.: 'Metamaterial-based efficient electrically small antennas', *IEEE Trans. Antennas Propag., 2006*, **54**, pp. 2113–2130

12 Landau, L.D., and Lifshitz, E.M.: 'Electrodynamics of continuous media' (Pergamon Press, Oxford, 1960), Sections, 61–64

13 Smith, D.R., and Kroll, N.: 'Negative refractive index in left-handed materials', *Phys. Rev. Lett.*, 2000, **85**, pp. 2933–2936

14 Tretyakov, S.A.: 'Electromagnetic field energy density in artificial microwave materials with strong dispersion and loss', *Phys. Lett. A*, 2005, **343**, pp. 231–237

15 Milonni, P.W.: 'Fast light, slow light and left-handed light' (IOP Publishing, London, 2005), Section 7.3

16 Caloz, C., and Itoh, T.: 'Electromagnetic metamaterials: transmission line theory and microwave applications' (Wiley-IEEE Press, Piscataway, NJ, 2005)

17 Scalora, M., D'Aguanno, G., Mattiucci, N., Bloemeri, M.J., Haus, J.W., and Zheltikov, A.M.: 'Negative refraction of ultra-short electromagnetic pulses', *Appl. Phys. B*, 2005, **81**, pp. 393–402

18 Skahill, G., Rudish, R.M., and Piero, J.: 'Electrically small, efficient, wide-band, low-noise antenna elements'. Proc. 1998 Antenna Applications Symp., Allerton Park, Monticello, IL, 16–18 September 1998, pp. 214–231

19 Chiao, R.Y., and Boyce, J.: 'Superluminality, paraelectricity, and Earnshaw's theorem in media with inverted populations', *Phys. Rev. Lett.*, 1994, **73**, pp. 3383–3386

20 Chiao, R.Y., Bolda, E., Boyce, J., Garrison, J.C., and Mitchell, M.W.: 'Superluminal and parelectric effects in rubidium vapor and ammonia gas', *Quantum Semiclassical Opt.*, 1995, **7**, pp. 279–295

21 Kuzmich, A., Dogariu, A., Wang, L.J., Milonni, P.W., and Chiao, R.Y.: 'Signal velocity, causality, and quantum noise in superluminal light pulse propagation', *Phys. Rev. Lett.*, 2001, **86**, pp. 3925–3928

22 Chen, Y.-F., Fischer, P., and Wise, F.W.: 'Negative refraction at optical frequencies in nonmagnetic two-component molecular media', *Phys. Rev. Lett.*, 2005, **95**, p. 067402

23 Ziolkowski, R.W., and Auzanneau, F.: 'Passive artificial molecule realizations of dielectric materials', *J. Appl. Phys.*, 1997, **82**, pp. 3197–3198

24 Auzanneau, F., and Ziolkowski, R.W.: 'Microwave signal rectification using artificial composite materials composed of diode loaded, electrically small dipole antennas', *IEEE Trans. Microw. Theory Tech.*, 1998, **46**, (11), pp. 1628–1637

25 Wittwer, D.C., and Ziolkowski, R.W.: 'Two time-derivative Lorentz material (2TDLM) formulation of a Maxwellian absorbing layer matched to a lossy media', *IEEE Trans. Antennas Propag.*, 2000, **48**, (2), pp. 192–199

26 Wittwer, D.C., and Ziolkowski, R.W.: 'Maxwellian material based absorbing boundary conditions for lossy media in 3D', *IEEE Trans. Antennas Propag.*, 2000, **48**, (2), pp. 200–213